LASER INTERFEROMETER GRAVITATIONAL WAVE OBSERVATORY
- LIGO -
CALIFORNIA INSTITUTE OF TECHNOLOGY
MASSACHUSETTS INSTITUTE OF TECHNOLOGY

Document Type **LIGO-T970149-00 - D** 11/2/96

Influence of the stray magnetic field generated by the Faraday isolator on SOS mirror actuators

Sanichiro Yoshida, Rana Adhikari, and David Reitze

Distribution of this draft:

This is an internal working note
of the LIGO Project.

California Institute of Technology
LIGO Project - MS 51-33
Pasadena CA 91125
Phone (818) 395-2129
Fax (818) 304-9834
E-mail: info@ligo.caltech.edu

Massachusetts Institute of Technology
LIGO Project - MS 20B-145
Cambridge, MA 01239
Phone (617) 253-4824
Fax (617) 253-7014
E-mail: info@ligo.mit.edu

WWW: http://www.ligo.caltech.edu/

1 Introduction

The Faraday isolator (FI) placed after the mode cleaner has a magnet that generates an intense B (magnetic) field. Part of this B-field leaks out of FI into surrounding areas. Because of the dynamic displacement of FI due to seismic noise, this stray B-field fluctuates with a frequency and amplitude determined by the combination of the seismic noise and the transfer function of the optical table on which FI is placed. This B-field fluctuation can affect the operation of the magnetic actuators used for nearby mirrors. In this note we consider how large this effect can be. We first compare this effect of FI with the influence of an ambient B-field considered by D. Coyne [1]. Then we make a more realistic estimation for the actuator magnets used for the last mirror of the mode cleaner, which is placed closest to FI in the current input optics design.

2 Explanation of the model and assumptions

2.1. System overview and coordinates definition

Figure 1 illustrates the coordinates used in the present model.The z axis is set along the optical axis where z=0 is set at the exit of FI. The y axis is coming out of the page perpendicularly. The FI magnet's dimensions are as shown in Table1. As a baseline for comparison with the IOO physical layout, we tilted the mirror by 45 deg to the optical axis.

2.2. Summary of assumptions

In this note, we made the following simplifying assumptions:

- FI's seismic vibration represents FI's relative motion to the actuator magnets.
- FI is placed on a vibration isolation stack using viton springs and FI's seismic vibration can be represented by the product of a horizontal ground-to-stack transfer function and ground noise. We use the horizontal ground-to-stack transfer function used by G. Gonzalez [2].
- The ground noise that the stack experiences can be represented by measured ground noise after removing the peak appearing at frequencies lower than ~0.1 Hz. Here the removal is to take into account the fact that the actuator and FI are placed close enough to ignore the low frequency component which are meaningful for much longer distances. We use ground noise measured at Livngston, LA [2] by cutting off the peak $>1\times10^{-6}$ m/Hz$^{0.5}$ around 0.1 Hz. (This corresponds to neglecting the wavelength microseismic motion.)
- The mirror has rotational freedom about its three principal axes as an cylinder.
- The stray B-field leaking from FI can be described by the B-field generated by a solenoid [3] that has the dimensions shown in Table1.
- The influence of FI stray B-field is assessed by comparing it with the open-loop displacement of the mirror that is evaluated as the product of a ground-to-stack transfer function, a stack-to-pendulum transfer function and ground noise. We use the same ground-to-stack transfer function and ground noise for the mirror as FI, and use the horizontal-to-horizontal, stack-to-pen-

dulum transfer function that S. Kawamura has calculated [4].

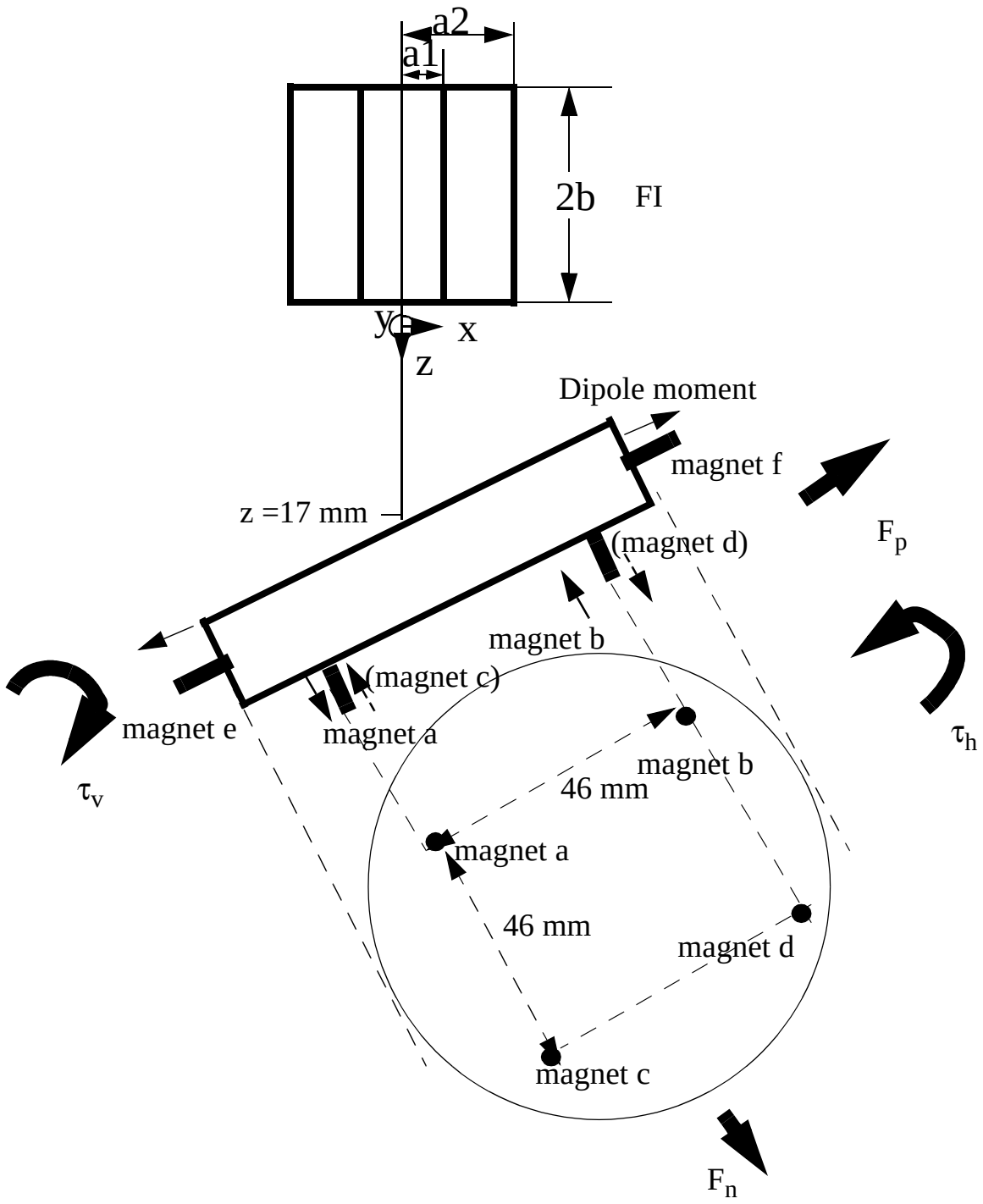

Figure 1: Faraday isolator and SOS actuator configuration. y axis is coming

out of the page. Thin arrows indicate the directions of dipole moments.

Table 1: FI magnet dimensions

Outer radius (a2)	Inner radius (a1)	Length (2b)	Field strength at center of magnet
25 mm	7.5 mm	60 mm	0.7 Ts

2.3. Force, torque and their temporal variations

Let $B(x, y, z)$ be the stray B-field. When the FI couples to seismic noise, the stray B-field varies as a function of time. To first order, its time derivative can be written as:

$$\frac{dB}{dt} = \frac{\partial B}{\partial x}\cdot\frac{dx}{dt} + \frac{\partial B}{\partial y}\cdot\frac{dy}{dt} + \frac{\partial B}{\partial z}\cdot\frac{dz}{dt} \tag{1}$$

where x, y, and z represent the frequency dependent seismic vibration of FI.

$$x(t) = \Delta x(\omega)\exp(i\omega t) \tag{2}$$

$$y(t) = \Delta y(\omega)\exp(i\omega t) \tag{3}$$

$$z(t) = \Delta z(\omega)\exp(i\omega t) \tag{4}$$

Substituting eqs. (2) - (4) into eq.(1), and integrating the result with respect to time, B becomes

$$B = B_0 + \left\{\frac{\partial}{\partial x}B_0\cdot\Delta x + \frac{\partial}{\partial y}B_0\cdot\Delta y + \frac{\partial}{\partial z}B_0\cdot\Delta z\right\}\exp(i\omega t) \equiv B_0 + B_1\exp(i\omega t) \tag{5}$$

where $B_0(x, y, z)$ is the static B-field that the actuator magnet would feel if FI was completely stationary.

The force F and torque τ that a magnet having a dipole moment μ feels can be written as

$$F = grad(\mu\cdot B) = grad(\mu\cdot B_0) + grad(\mu\cdot B_1)\exp(i\omega t) \equiv F_0 + F_1\exp(i\omega t) \tag{6}$$

and

$$\tau = \mu\times B = \mu\times(B_0 + B_1\exp(i\omega t)) \equiv \tau_0 + \tau_1\exp(i\omega t) \quad , \tag{7}$$

respectively.

Thus if B is given as a function of x, y, and z, F and τ can be evaluated from eqs. (6) and (7). F_0 and τ_0 are the static force and torque that the actuator magnet feels due the presence of the FI, and F_1 and $\tau_1$are the amplitude of the temporal fluctuation of the force and torque caused by seimic noise. We call B_0, F_0 and τ_0 the static component, and B_1, F_1 and τ_1 the dynamic component.

2.4. Stray B-field

We contacted several FI manufacturers to ask for the spatial distribution of the stray B-field. One manufacturer among them who has over twenty-year experience of developing low leakage B-field FIs provided most substantial information. According to this manufacturer [5] their new model FI has been designed to have minimum B-field leakage. They say that because of this special design to suppress the stray B-field, its spatial dependence cannot be expressed analytically, and therefore, they have calculated the z dependence of B numerically. For proprietary reasons, they do not disclose the numerical solution except for the facts that at the far field (z>8*outer diameter of the FI magnet =0.25 x 8 = 20 cm, in our case) the B-field attenuation has z/d_{ap}^{-4} dependence on the optical axis where d_{ap} is the clear aperture and z is the coordinate along the optical path, that the B-field at the center of the magnet is 0.7 T, that the field decays radially much faster than along the optical axis, and that their new model FI's B-field decays much faster than their old model FI. They disclosed that their old model FI is well approximated by a solenoid. Other manufactures said that the B-field of their own FIs can be well approximated by a solenoid. For these reasons, we used the solenoid model in this estimation. The figure below compares the decay of the new FI and old FI. Note that both in the B-field and its slope, the solenoid model is larger than the New FI model. Our estimation, therefore, is in the safe side.

Assuming a solenoid having the dimensions shown in Table1 for the FI magnet, the stray B-field can be written as [3]

$$B_x(x,y,z) = 3x \cdot B_a(z+b) \cdot \frac{(z+b)^4}{((z+b)^2+(x+y)^2)^{5/2}} \tag{8}$$

$$B_y(x,y,z) = 3y \cdot B_a(z+b) \cdot \frac{(z+b)^4}{((z+b)^2+(x+y)^2)^{5/2}} \tag{9}$$

$$B_z(x,y,z) = \frac{1}{2} \cdot B_a(z+b) \cdot \frac{(z+b)^3}{((z+b)^2+(x+y)^2)^{3/2}} \left(\frac{3(z+b)^2}{(z+b)^2+(x+y)^2} - 1 \right) \tag{10}$$

where B_x, B_y and B_z are the x, y, and z components of the static stray B-field B_0, respectively, B_a is the B-field strength along the z axis, b is a half of the FI magnet's length and (x, y, z) is set as shown in Fig.1. Fig.2 shows the on-axis B-field B_a that we use in this estimation.

.

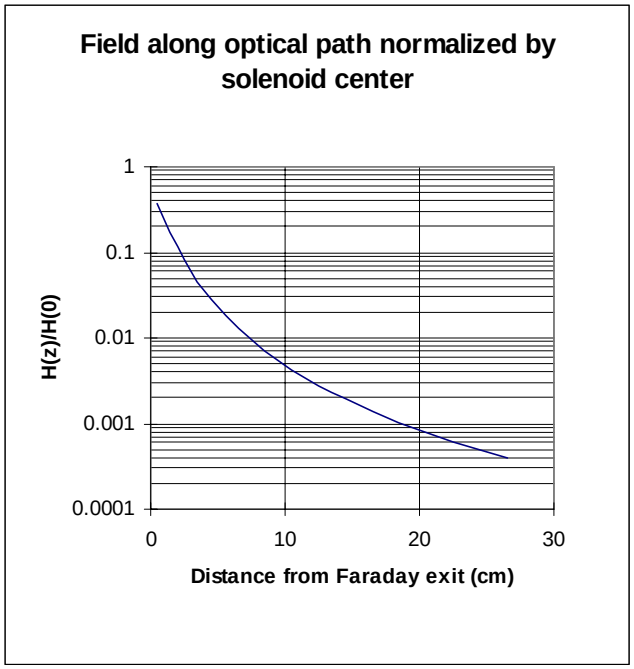

Figure 2: On-axis B-field used in this estimation

2.5. FI's seismic vibration

The FI's vibration due to seimic noise can be estimated as a function of frequency by multiplying the ground vibration and the transfer function. Fig.3 shows the FI's vibration used in this estimation.We estimated the FI's displacement by multiplying the ground noise (see Fig.4 of Ref [2]) and horizontal ground-to-stack transfer function (see Fig. 13 of Ref. [2]), whereas the SOS open-loop noise by multiplying the same ground noise, the same ground-to-stack transfer function and the stack-to-pendulum transfer function (horizontal to horizontal) [4]. To consider only short range ground noise influences, we cut off the microseismic peak appearing 0.1 - 0.3 Hz in Fig.4 of Ref. [2] and replaced it by a constant value of $1x10^{-6}$ m /$Hz^{0.5}$.

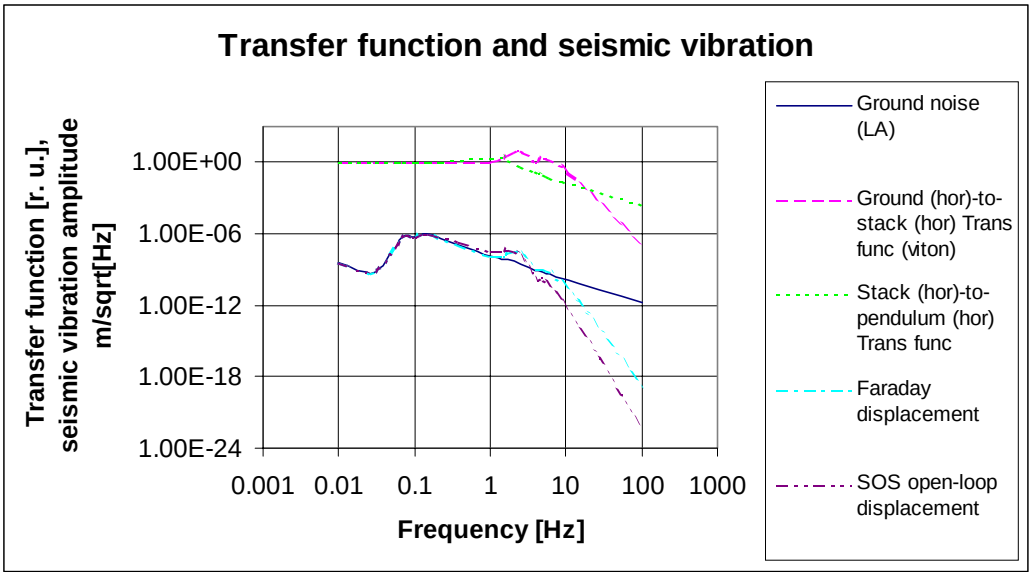

Figure 3: Ground noise, transfer functions and resultant seismic vibrations used in this estimation.

3 Calculations

Now that B_0 is given by eqs.(8) - (10) as an explicit function of space, the force, torque and their temporal fluctuations can be estimated from eqs. (5) - (7) for a given magnet, where the amplitude of the seismic vibration of the FI from Fig.3 are used for Δx, Δy and Δz in eq.(5). Then with the calculated forces and torques the actual displacement of the mirror can be estimated using an appropriate equation of motion. Below we first consider the displacement of a large mirror actuated by a single magnet operating under the influence of the stray B-field, and compare the result with the Coyne's calculation in which he estimated the displacement of the same mirror due to the torque caused by an ambient B-field internal to the chamber and that due to the force caused by the gradient of the ambient B-field [1]. Then we estimate the displacement of a small mirror actuated by six magnets in a realistic configuration. Here the large and small mirrors mean the large and small optics used in LIGO [6].

3.1. Single actuator magnet case and comparison with the effect of an ambient B-field (for a large mirror)

Prior to the estimation of the mirror displacement, we calculate F_0 F_1 τ_0 and τ_1 that a single actuator magnet feels when its dipole moment vector is oriented at 45 degree to the optical axis. Figs. 4 - 6 respectively show x, y, and z components of the static force and torque F_0, τ_0, and the amplitude of the dynamic component F_1 and τ_1 calculated for an actuator magnet placed on a plane y=23 mm as a function of x and z. This height of 23 mm is a realistic number for actuator magnets used in LIGO [6].

For this calculation we used the nominal dipole moment of 0.0107 A m^2 used by Coyne [1] and the maximum seismic vibration amplitude of 10^{-6} m observed in Fig. 2. Figs. 4 - 6 show that while both the static and dynamic components decay quickly as going away from the FI, a considerable level remains at x<5 cm where actuator magnets are designed to be placed [6].

We next estimate the displacement of a mirror caused by the dynamic components of the force and torque. To compare the result with the Coyne's estimation on the effect of an ambient B-field, we use a large mirror in this estimation. Following the Coyne's calculation, we evaluated the displacements due to the force and torque to the actuator magnet as a sinusoidal response; i.e., $\delta_x^t = F_x / 20\, M_l \omega^2$, $\delta_y^t = F_y / 20\, M_l \omega^2$, $\delta_z^t = F_z / 20\, M_l \omega^2$, and $\delta_x^r = d_{off}\, \tau_x / 20\, I_l \omega^2$, $\delta_y^r = d_{off}\, \tau_y / 20\, I_l \omega^2$, $\delta_z^r = d_{off}\, \tau_z / 20\, I_l \omega^2$, where the superscripts t and r denote the displacement due to the translational and rotational motion, respectively, M_l and I_l are the mass and moment-of-inertia of the large mirror, d_{off} is the incident beam offset for the large mirror [1] and 20 is the safety factor from SYS requirements. (Coyne uses the factor of 20 in the denominators of $\delta x^t = F_x / M_l \omega^t$, $\delta y^t = F_y / M_l \omega^2$, etc., so did we.) We evaluated the moment-of-inertia by assuming that the mirror is a cylinder;

$$I = M \cdot \frac{r^2}{4} + M \cdot \frac{l^2}{12} \tag{11}$$

where M, r and l are, respectively, the mass, radius and thickness of the cylinder. Table 2 summarizes the values we used for this calculation (see the row for the large mirror). Fig.7 and 8 compare the calculated displacements with the displacements due to the ambient B-field [1]. When the mirror is 20 cm away from the FI along the optical axis, the resultant displacement is comparable (to a factor of 10) or smaller than the displacement due to the ambient B-field. Note that it is more than several orders of magnitude lower than the ambient field case in the gravitational wave band (>40 Hz). When the mirror is 50 cm away, the calculated displacements are lower than the ambient field case in the whole frequency range. Table 3 summarizes the calculated dynamic forces and torques felt by the single magnet as a function of the distance from the FI, *z* (cm).

Table 2: Mirror dimensions

	Diameter	Thickness	Weight	Moment of inertia	Beam offset d_{off}
large mirror	25.4 cm	10 cm	10 kg	0.0391458 kg m^2	1 mm
small mirror	7.62 cm	2.5 cm	0.25 kg	0.0001042 kg m^2	3 mm

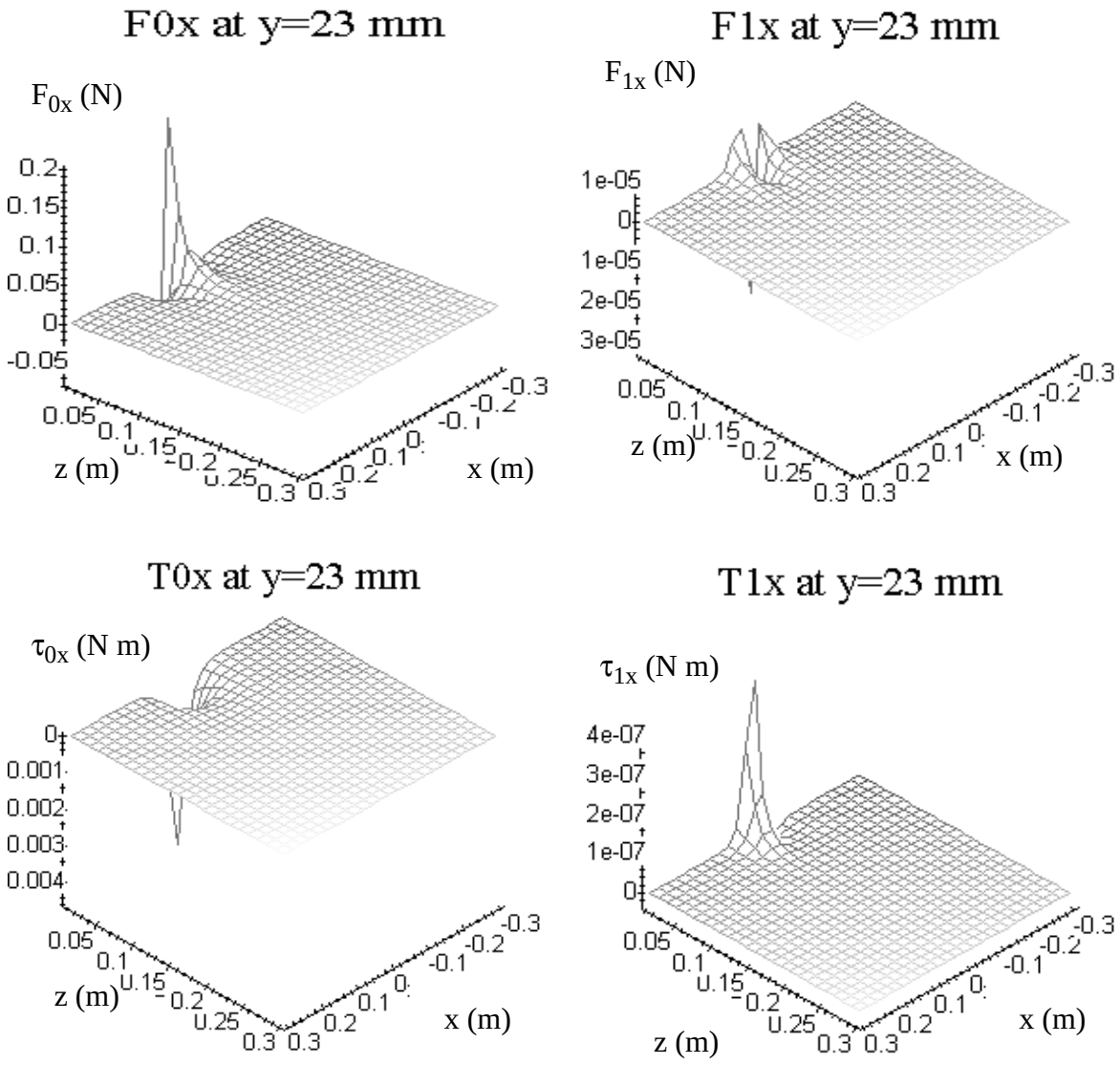

Figure 4: Calculated force and torque felt by a single magnet (x components)

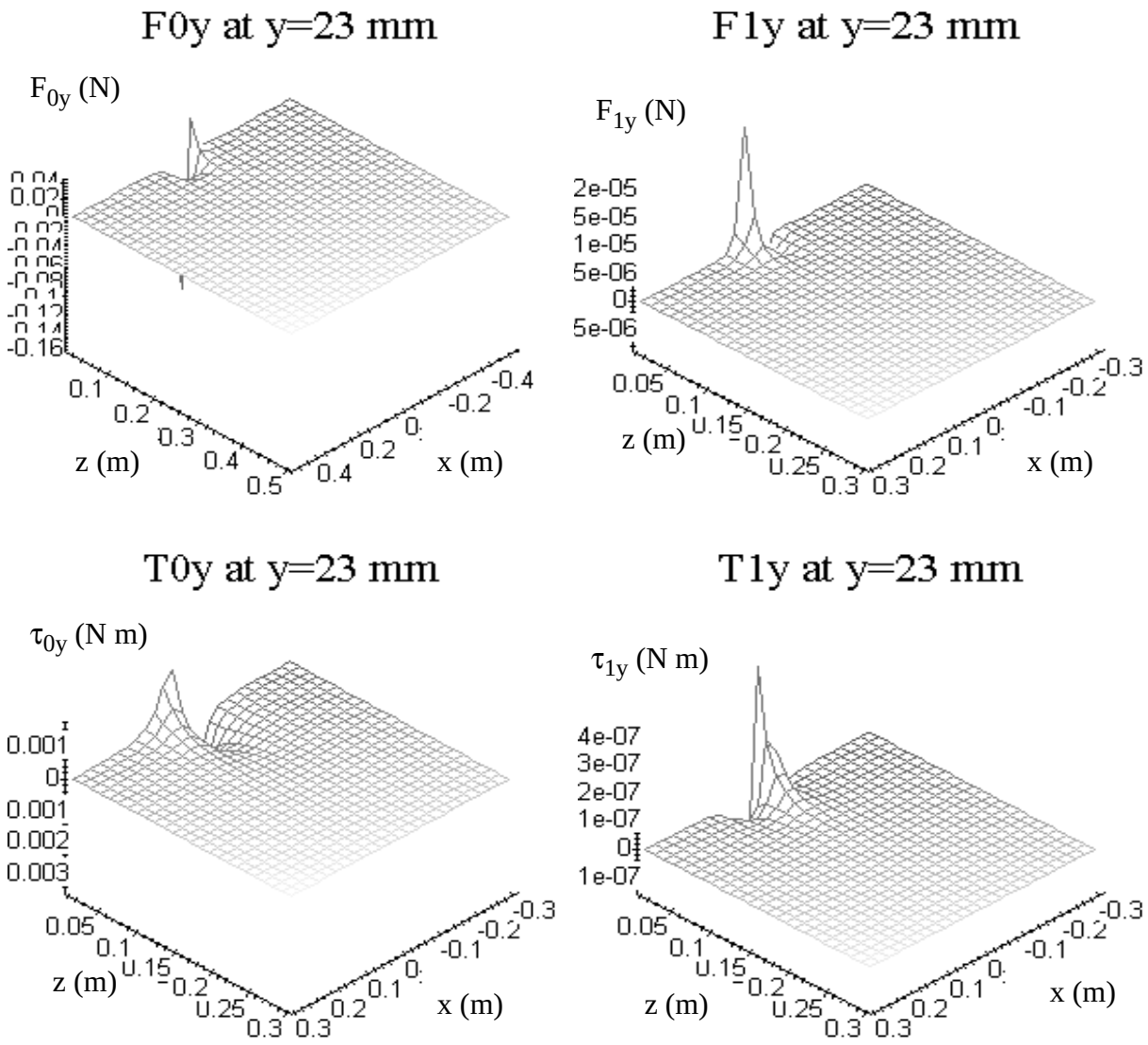

Figure 5: Calculated force and torque felt by a single magnet (y components)

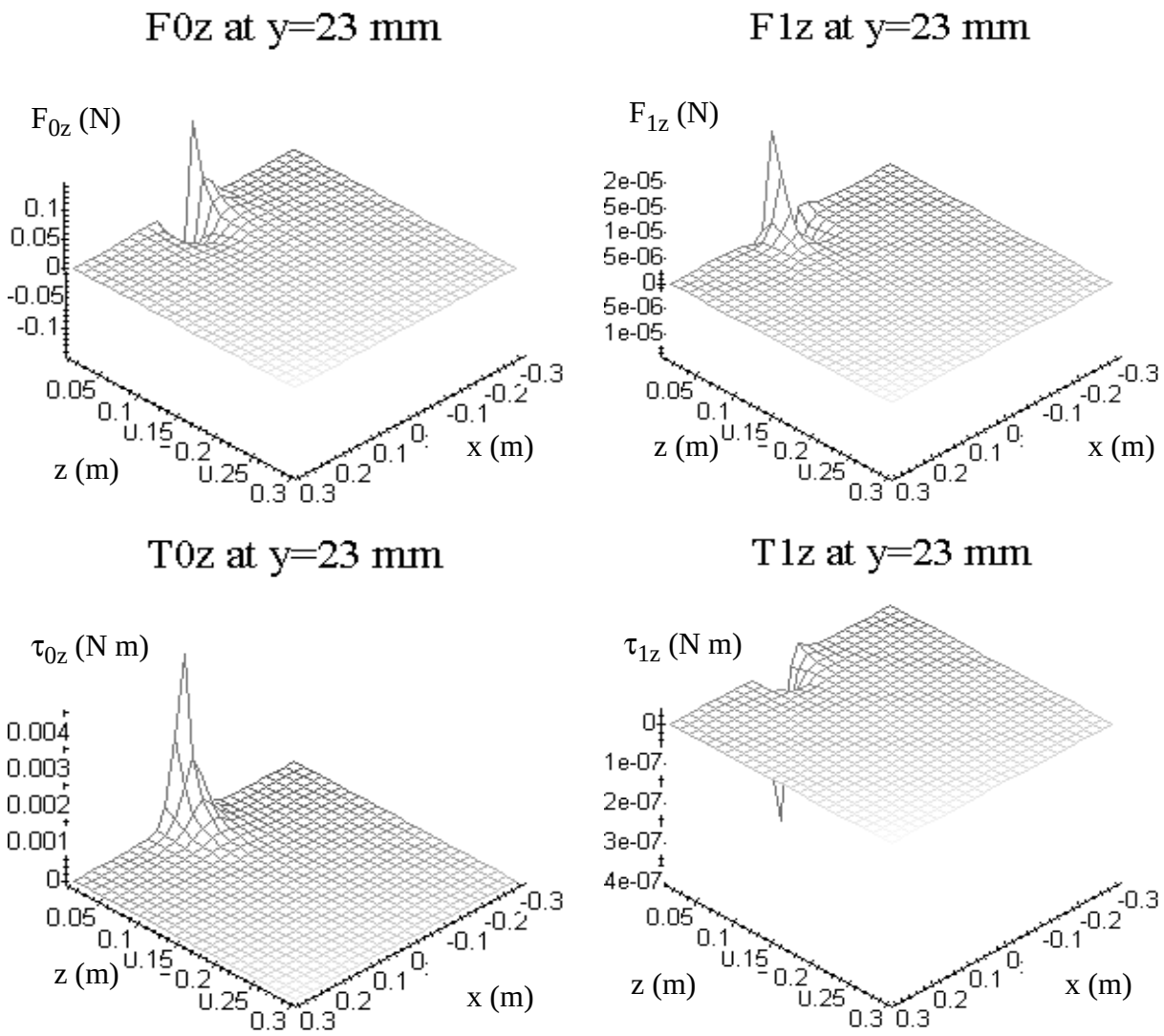

Figure 6: Calculated force and torque felt by a single magnet (z components)

Table 3: Dynamic components of force and torque around 0.1 Hz (single magnet case)

z (cm)	F_{1x} (N)	F_{1y} (N)	F_{1z} (N)	τ_{1x} (Nm)	τ_{1y} (Nm)	τ_{1z} (Nm)
20	-1.82e-9	-1.92e-9	-3.36e-10	-4.19e-10	3.44e-10	-7.46e-11
50	-2.70e-11	-2.74e-11	-1.22e-11	-1.42e-11	8.45e-11	-1.19e-11
100	-9.55e-13	-9.58e-13	-5.27e-13	-9.75e-13	9.37e-13	3.80e-14

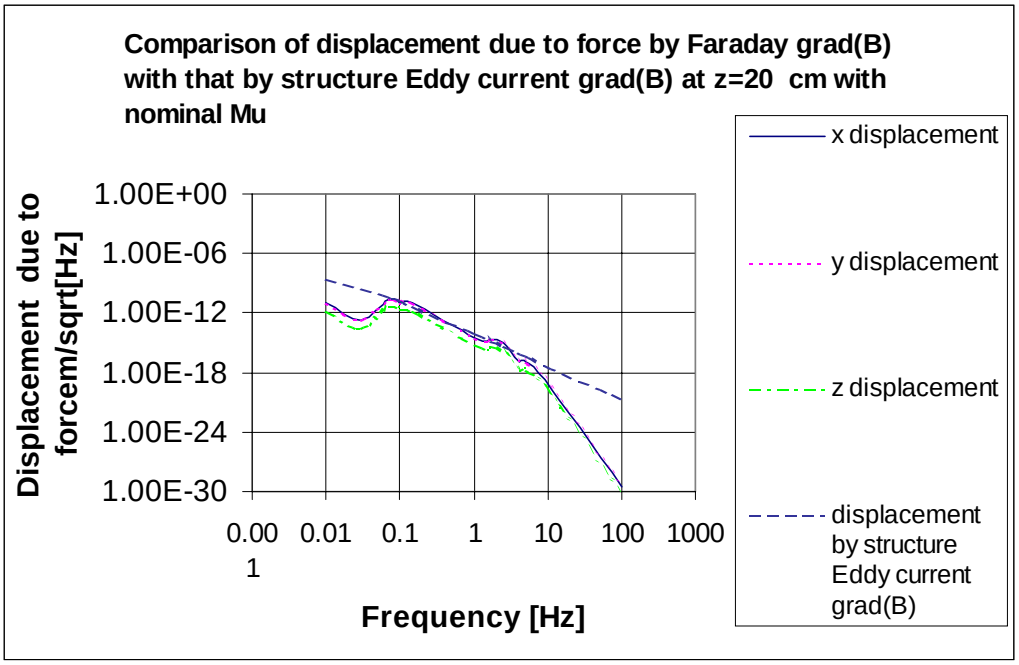

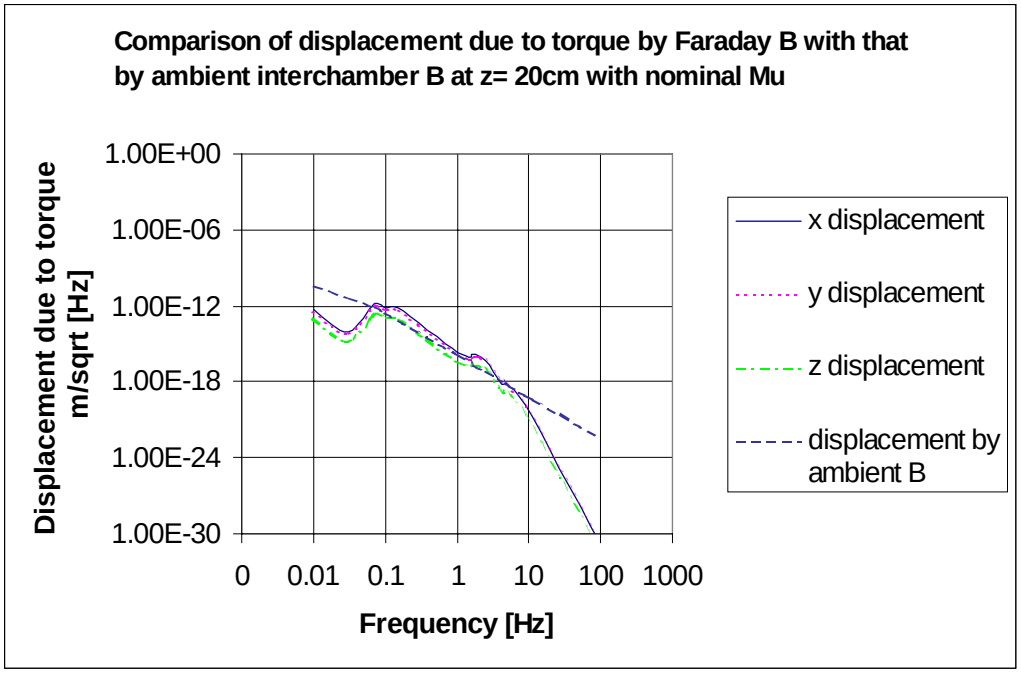

Figure 7: Comparison of displacement due to FI stray B-field with displacement due to force by ambient B-field gradient (upper) and displacement due to torque by ambient B-field (lower). LOS actuator is placed 20 cm from FI.

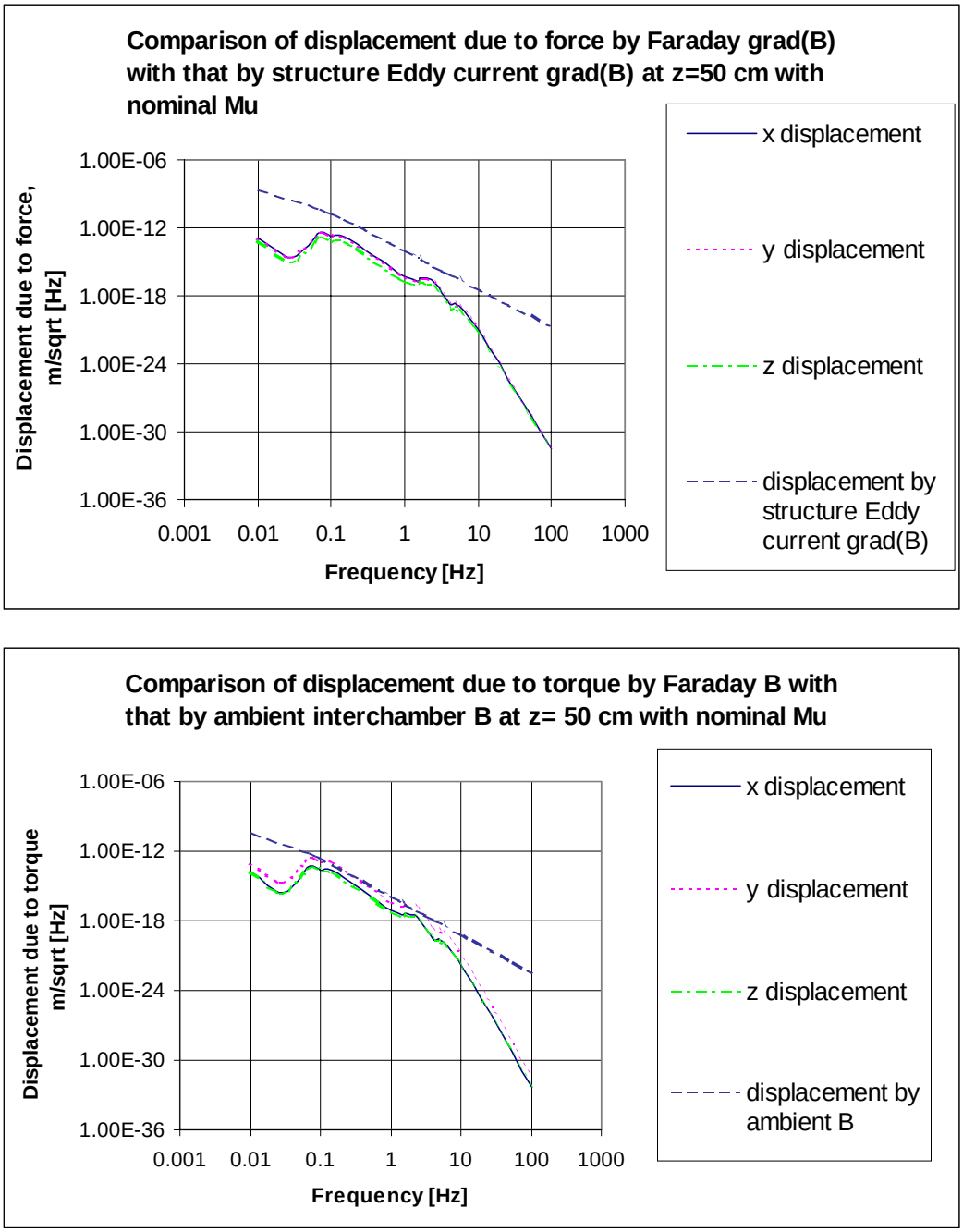

Figure 8: Comparison of displacement due to FI stray B-field with displacement due to force by ambient B-field gradient (upper) and displacement due to torque by ambient B-field (lower). LOS actuator is placed 50 cm from FI

3.2. Realistic actuator magnets arrangement (small mirror)

Next, we estimate the displacement of a small mirror under the configuration shown in Fig.1. We considered all the dynamic components of the forces and torques felt by the six magnets (F_{1x}, F_{1y}, F_{1z}, τ_{1x}, τ_{1y} and τ_{1z} for magnet a through f) to derive translational and rotational equations of motion and solved them for displacements normal and parallel to the mirror surface due to translational motion, and displacements due to horizontal and vertical rotational motion of the mirror. For these calculations, we used the same frequency response as the above-shown single actuator magnet case but did not use the safety factor of 20; i.e., $\delta_n{}^t = F_n/M_s\omega^2$, $\delta_p{}^t = F_p/M_s\omega^2$, $\delta_v{}^t = F_v/M_s\omega^2$, $\delta_h{}^r = d_{off}\,\tau_h/I_s\omega^2$, $\delta_v{}^r = d_{off}\,\tau_v/I_s\omega^2$. Here subscripts n, p, v and h denote normal to the mirror surface, parallel to the mirror surface, vertical and horizontal, respectively, M_s and I_s are the mass and moment-of-inertia of the small mirror, F_k and τ_k *(k=n, p, h, v)* are the total forces and torques in the respective directions, and d_{off} is the incident beam offset for the small mirror [7]. Table 4 shows the static and dynamic forces and torques calculated for each magnet together with the total values at around 0.1 Hz where the FI vibration is at its maximum.

Table 4: Static and dynamic force and torque at around 0.1 Hz (realistic case)

	a	b	c	d	e	f	total
F_{0n} (N)	2.298e-5	2.627e-4	-2.298e-5	-2.627e-4	-3.551e-4	7.803e-4	4.251e-4
F_{0p} (N)	3357e-4	-6.458e-4	-3.357e-4	6.458e-4	1.348e-4	4.881e-4	6.229e-4
F_{0v} (N)	-4.611e-5	1.321e-4	-4.611e-5	1.321e-4	0	0	1.720e-4
τ_{0h} (Nm)	1.959e-5	1.558e-5	1.959e-5	-1.558e-5	1.083e-5	-6.452e-5	-1.010e-4
τ_{0v} (Nm)	-7.940e-6	1.400e-5	-7.940e-6	1.400e-5	0	0	2.028e-5
F_{1n} (N)	-4.636e-9	1.651e-10	5.240e-9	-4.225e-9	5.234e-9	-3.310e-8	-3.132e-8
F_{1p} (N)	-5.022e-9	1.815e-8	2.814e-9	-1.248e-8	-7.106e-9	-1.603e-9	-5.249e-9
F_{1v} (N)	-1.424e-9	2.304e-9	2.280e-9	-8.046e-9	-2.636e-8	4.817e-9	-2.706e-9
τ_{1h} (Nm)	5.465e-10	-7.332e-10	-4.441e-10	6.085e-10	1.646e-10	8.400e-10	2.788e-9
τ_{1v} (Nm)	-1.922e-10	2.391e-10	-4.634e-10	-8.968e-10	0	0	-6.542e-10

Fig. 9 shows the resultant displacements when the small mirror is 17 cm away (taken from an early version of the IOO optics layout) from the FI (see Fig.1) and compare them with the open loop displacement noise of SOS. Here, the open loop noise is evaluated by multiplying the above-used ground noise, the above-used ground-to-stack transfer function and the horizontal-to-horizontal, stack-to-pendulum transfer function evaluated by S. Kawamura [4]. Because the stack that the FI is placed has no active control to compensate the seismic noise, this comparison with an open loop displacement of the small mirror is reasonable. When we use the above-used nominal dipole moment 0.0107 A m^2, the calculated displacements are orders of magnitude smaller than the SOS open loop displacement in the frequency region higher than 0.1 Hz, and comparable with it at the lower frequency region. *This means that the displacement due to the FI stray B-field should be compensated by the SOS actuator.* In Fig.9, the calculated displacement due to the FI when FI is 30 cm away from the SOS is also shown. In this case, the displacement due to the FI is smaller than the SOS open loop displacement in the whole frequency region considered.

A comparison of Fig.9 (upper graph) with Fig.7 (upper graph) around 0.1 Hz indicates that the displacement calculated in the realistic six magnet configuration for the small mirror is four orders of magnitude higher than the displacements caused by the force for the single magnet on the large mirror. Note that this difference comes from the following factors:i.e., the ratio of the large mirror mass to the small mirror mass=10 kg/0.25 kg = 40, the safety factor of 20 used only in the single magnet case, and the ratio of the force felt by the single magnet to the total force by the six magnets=$3x10^{-7}$ N/$1.8x10^{-8}$ N=16 (see F_{1n} total in Table 4 and F_{1x} in Table 3); overall difference = 40 x 20 x 16=$1.2x10^4$. The five-orders-of-magnitude difference between the displacements in the realistic case (Fig.9, upper graph) and the displacements caused by the torque for the single magnet (Fig.7 lower graph) can be explained in the same way by considering that the ratio of the large mirror moment-of-inertia to the small mirror moment-of-inertia is 0.0391458 kg m^2/0.0001042 kg m^2 =376, therefore the overall difference is 40 x 20 x 376=$3x10^5$. Also note in Table 4 that the total F_{1n} is dominated by magnet f that is placed closest to FI. These mean that the difference in the resulting displacement between the single magnet case and the realistic six magnet case is mostly due to the difference in the mirror size and the safety factor, and partly due to some magnets placed close to FI.

3.3. Orientations of SOS magnets and mirror (small mirror)

Finally, we examine if the displacements are sensitive to the orientations of the SOS magnets and the mirror. Thus we considered the following two cases: (i) we arranged the SOS magnets in such a way that the four magnets attached to the rear of the mirror and the two magnets attached to sides of the mirror, respectively, have the same orientations of the dipole moments; (ii) we rotated the whole mirror horizontally such that the incident angle of the laser beam might be 0 and 90 deg. In all the cases, the SOS magnet's dipole moment is the above-used nominal value, and the mirror is placed 17 cm from the FI.

Fig.10 summarizes the results, where the top graph is the case when the SOS magnets are arranged non-alternatively, and the middle and bottom graphs are the cases when the mirror is rotated so that the incident angle may be 0 and 90 deg. In either case, no substantial difference is

observed as compared with Fig.9 upper graph where the SOS is placed 17 cm away from FI with the beam incident angle of 45 degree and the SOS magnets are oriented alternatively.

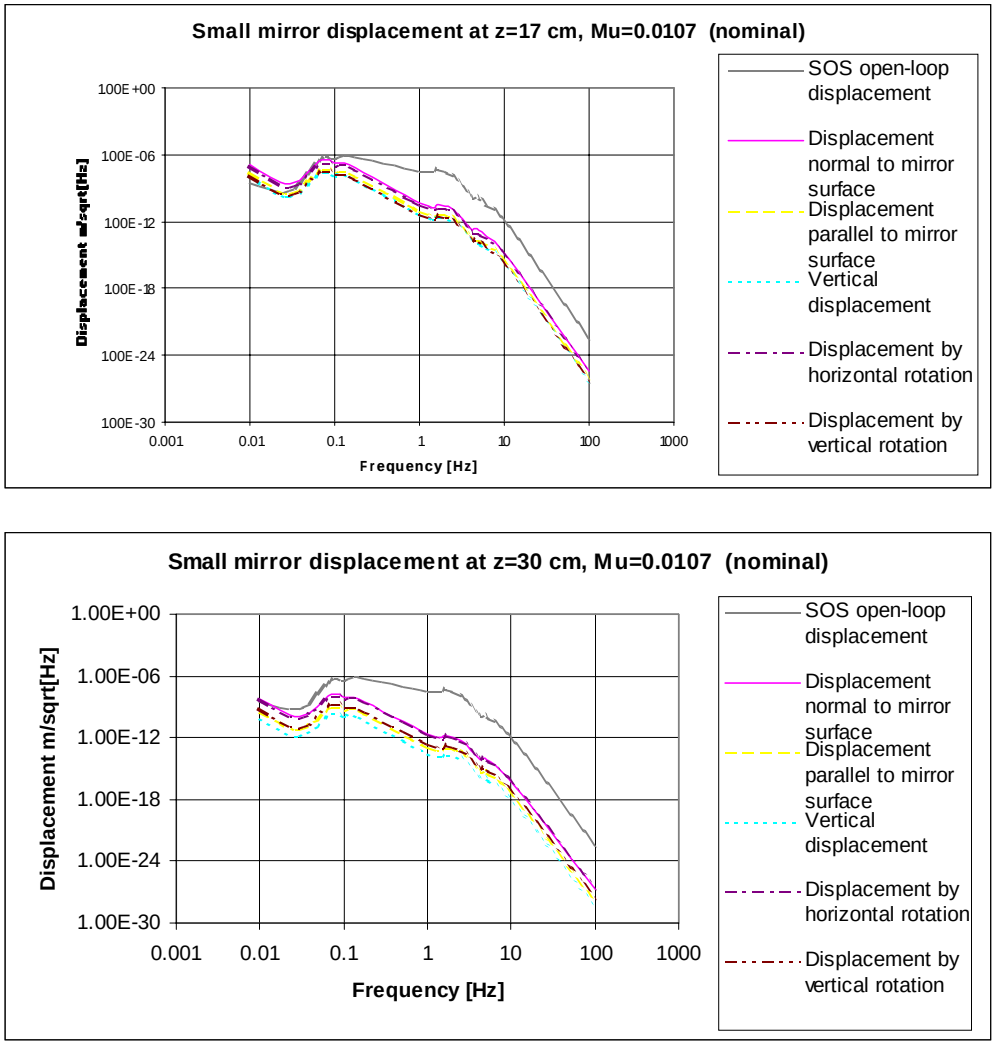

Figure 9: Displacement of small mirror in a realistic SOS configuration with six magnets of nominal dipole moment when SOS is placed 17 cm (upper) and 30 cm (lower) from FI.

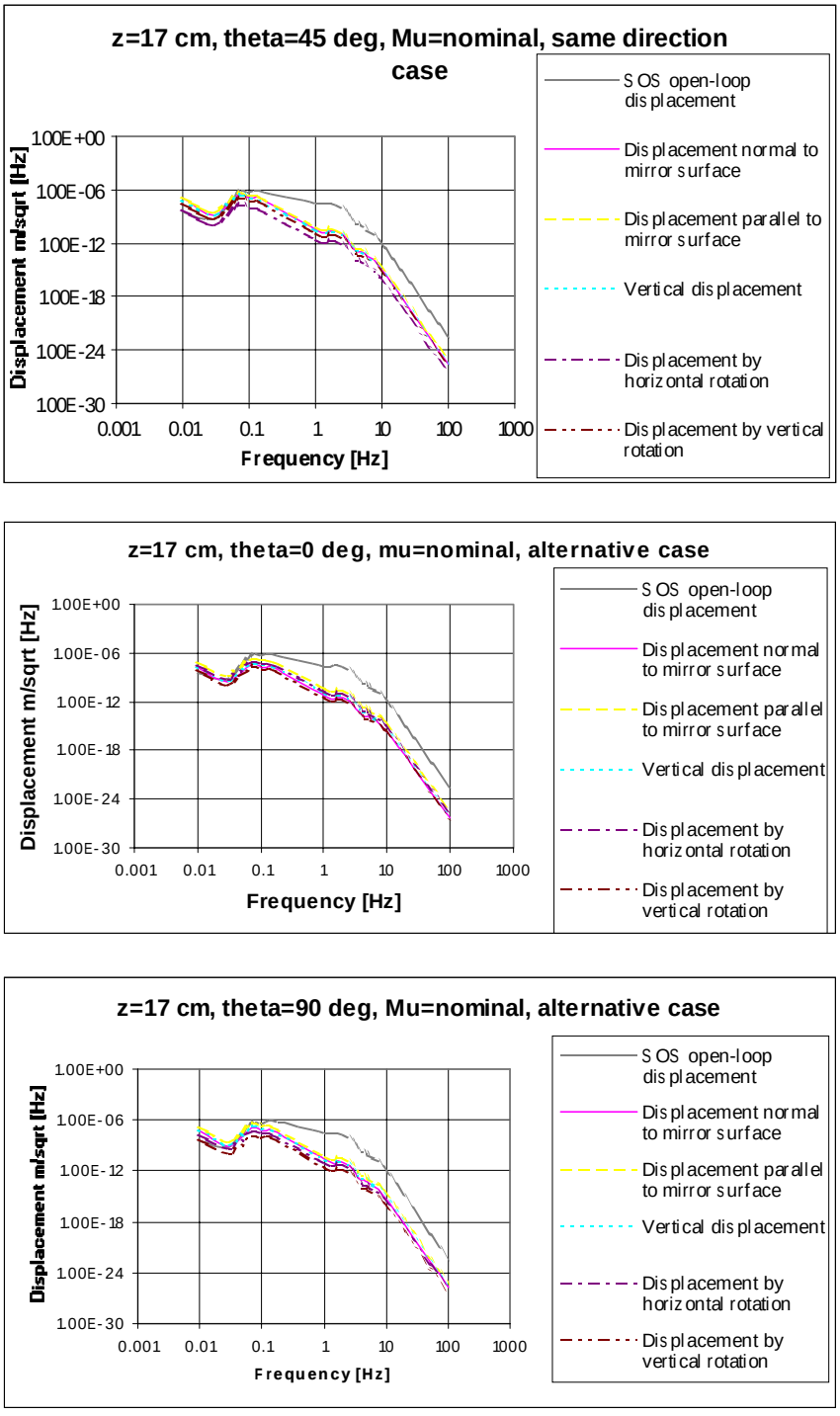

Figure 10: Calculated displacements for various cases; (top graph): SOS at z=17 cm from FI, SOS magnets orientation = same orientation, beam incident angle θ = 45 deg; (middle graph): z=30 cm, magnets = alternatively, θ = 0 deg, (bottom graph): z=17 cm, magnets = alternatively, θ = 90 deg. All magnets has mu nominal.

4 Conclusions

This calculation shows that as far as the current optical configuration is concerned, the displacement of the small mirror due to the combined effect of FI stray B-field and FI's seismic motion should be compensated by the SOS mirror actuators. It is also shown that the displacements are not sensitive to the SOS magnets and the angle of the mirror to the optical axis

References:

[1] D. Coyne, Magnetic Dipole Moment Limits, 8/29/96

[2] G. Gonzalez, ASC: Environmental Input to Alignment noise, LIGO-T960103-00-D, July 1996

[3] D. Bruce Montgomery, "Solenoid Magnet Design", Wiley-Interscience, p.226 - 243 (1969)

[4] S. Kawamura, Response of Pendulum to Motion of Suspension Point, LIGO-T960040-00-D, Mar. 11, 96

[5] Tech Plus, 6709 La Tijera Blvd, Los Angeles, CA 90045, (ph) 213-296-1182

[6] S. Kawamura, J. Hazel and F. Raab, Suspension Preliminary Design, LIGO-T960074-07-D, Dec. 3, 96

[7] S. Kawamura and F. Raab, Suspension Design Requirements, LIGO-T950011-17-D, July 2, 97